Wheat responds to lack of root hairs with recruitment of bacteria harboring P mineralization genes and increased arbuscular mycorrhizal fungi arbuscularisation

Courtney Horn Herms[1], Ian Tsang[2,3], Frederik Bak[1], Klara Gunnarsen[1], Magdalena Hasenzagl[1], Amaru Miranda Djurhuus[1], Tom Thirkell[4], Eric Ober[2], Fiona Leigh[2], James Cockram[2], Mette Haubjerg Nicolaisen[1]

1) Department of Plant and Environmental Sciences, University of Copenhagen, Thorvaldsensvej 40, 1871 Frederiksberg, Denmark

2) Niab, Park Farm, Histon, Cambridge, CB24 9NZ, United Kingdom

3) School of Biosciences, University of Nottingham, Sutton Bonington, Loughborough LE12 5RD, United Kingdom

4) Department of Plant Sciences, University of Cambridge, Cambridge, CB3 0LE, United Kingdom

Corresponding Author: Mette Haubjerg Nicolaisen; email: meni@plen.ku.dk

ORCIDs: C.H.H.: 0000-0002-7363-3189; I.T.: 0009-0006-1999-3251; F.B.: 0000-0001-9580-8018; K.G.: 0000-0001-8176-8844; M.H.: no ORCID; A.M.D.: 0000-0003-3762-2922; T.T.: 0000-0002-4481-0924; E.O.: 0000-0002-4832-5897; F.L.: 0000-0002-3221-5327; J.C.: 0000-0002-1014-6463; M.H.N.: 0000-0002-0983-2466

Summary

- Plant roots simultaneously rely on root hairs and the rhizosphere microbiome to acquire poorly accessible P from the soil, but the full potential of the plant to utilize its microbiome for nutrient capture has yet to be fully understood. We hypothesized that a wheat mutant defective in root hair elongation could recruit more P-cycling bacteria and AMF compared to its wild-type background to compensate for the loss of root hairs.
- Through quantitative polymerase chain reaction and arbuscular mycorrhizal fungi (AMF) staining, we quantified the enrichment of bacterial P-cycling genes and AMF colonization across different stages of wheat development and in differentially P fertilized soils in the presence and absence of root hair elongation.
- The loss of root hair elongation led to an enrichment of P-cycling bacteria during very early seedling development, where P mineralizing bacteria dominated over P solubilizing bacteria. The AMF symbiosis was only fully established after several weeks

of growth, but then arbuscularisation became dominant over bacterial P mineralization in the root hair mutant.

- Wheat can recruit and rely on bacterial P mineralization to meet their P needs before the AMF symbiosis is fully dominant and then release these bacteria once the AMF symbiosis is developed.

Key Words

Arbuscular Mycorrhizal Fungi (AMF), Phosphorus (P) cycling, plant-microbe interactions, rhizosphere microbiome, root hairs, *Triticum aestivum* (wheat)

Introduction

Agricultural productivity is primarily constrained by nutrient availability. Phosphorus (P) is an essential nutrient and vital for central biochemical processes in the plant (Rengel et al., 2022). However, despite a relatively large amount of total P in many soils, bioavailable P is often limited in the soil environment, restricting plant growth and yield (Menezes-Blackburn et al., 2018). Thus, P is one of the most heavily applied nutrients to agricultural fields, but P fertilizer is poorly absorbed by the plant (Simpson et al., 2011), leading to environmental degradation via eutrophication (Ulén et al., 2007). Furthermore, raw phosphate rock used to make P fertilizer is a finite resource with high energy demands for production (Van Kauwenbergh, 2010), further impacting the sustainability of current P fertilization practices. As the need to grow more food using reduced inputs becomes critical to future food security, research is increasingly focusing on ways to improve crop P nutrition under reduced chemical inputs.

Recently, belowground plant traits have become a focus for the improvement of plant nutrition under low fertilizer input (Ober et al., 2021). For example, root hairs elongate under low-P conditions and help the plant access great volumes of soil, improving access to nutrients (Bates & Lynch, 1996; Tsang, Atkinson, et al., 2024). However, increasing root hair length has a maximum capacity to improve plant P uptake, and further augmentation may lead to negative pleotropic effects such as reduced aboveground biomass (Brown et al., 2012; Zhang et al., 2018). Other mechanisms for plant nutrition that complement root function and performance will therefore need to be integrated into future crops.

Improving beneficial interactions between the plant and its microbiota is another promising target for sustainable plant nutrient uptake (Ge & Wang, 2025). The microbiome of the soil influenced by plant roots, termed the rhizosphere, contains many vital functions for crop health, including P acquisition. Symbiotic arbuscular mycorrhizal fungi (AMF) are especially important for plant P uptake (Smith & Smith, 2011), also in globally important crops such as wheat (*Triticum aestivum* L.) (Thirkell et al., 2020). When lacking P, plants can selectively boost colonization by AMF to increase their P uptake (Kumar et al., 2019; Zhou et al., 2022). The bacterial fraction of the rhizosphere microbiome also carries functions relating to the cycling of both organic and inorganic P (Bergkemper et al., 2016). Single bacterial isolates demonstrate the ability to increase crop P nutrition and have been suggested as promising bio-based fertilizers (Azaroual et al., 2020; Jensen et al., 2024). However, compared to AMF, much less is known about the ability of the plant to actively enrich and utilize bacterial communities to increase P nutrition.

Unraveling how plants enrich both AMF and bacteria to improve P nutrition may inform strategies to leverage plant-microbe interactions under reduced agricultural inputs. However,

it has not been shown that crops can enrich bacteria with P-cycling abilities in the rhizosphere in times of need, potentially due to the dominance of other mechanisms for P uptake, namely the elongation of root hairs (Bates & Lynch, 1996). In this work, we used the recently developed wheat (*Triticum aestivum* L.) root hair mutant *short root hair 1* (*srh1*) (Tsang, Thomelin, et al., 2024) to assess the ability of wheat to leverage the soil microbiome for P nutrition when root hair elongation, the dominant plant response to P limitation which can otherwise obscure this interaction, is absent. We hypothesized that the root hair mutant would recruit more P-cycling bacteria and AMF compared to its wild-type background to compensate for the loss of root hairs. The aims were investigated via two principal experiments. First, a field experiment compared the development of the P-cycling bacterial community and AMF colonization with and without the presence of root hairs under field conditions. Second, a pot experiment using contrasting high- and low-P soils was used to compare the status of the P-cycling bacterial community and AMF symbiosis at booting, when P uptake is highest (Jones et al., 2024), in the root hair mutant and wild-type. Long-read 16S ribosomal RNA (rRNA) amplicon sequencing complemented the quantitative polymerase chain reaction (qPCR)-based functional analyses of the bacterial microbiome, while AMF were quantified through qPCR and traditional staining.

Materials and Methods

Plant material

The wheat root hair mutant, *srh1,* and its wild-type derived line are previously described (Tsang, Thomelin, et al., 2024). Briefly, the mutant was identified by Tsang et al. (2024) in a forward screen of an ethyl methanesulfonate (EMS) mutated population created in the spring wheat cultivar Cadenza (Krasileva et al., 2017). In the mutant, root hairs initiate but fail to elongate.

Field experiment set-up and sampling

Wild-type and mutant seeds were sown in spring 2024 in a complete randomized block design in Hinxton, Cambridgeshire, United Kingdom (52°05'56.1"N, 0°10'41.8"E). The field soil characteristics are described in Table S1. Approximately 120-180 seeds were sown per plot, where each plot measured 1x1 m with 6 rows of plants per plot. At two and four weeks post-sowing (GS11 and GS12-GS13, respectively; Zadoks et al., 1974), one individual plant was dug up from each replicate plot (n=10) using a sterilized shovel. The shoot length and the length of the longest root of the root system were measured, and samples were taken in the field as described by Guan et al. (2024). As the field-grown rhizoplane (soil directly attached to the root) was too small to sample, only the rhizosphere (soil influenced by the root) sample was taken. At each sampling time point, bulk soil (n=5) was also collected from the bare soil

between the plots. Samples were stored at -80 °C until freeze-drying under vacuum at -70 °C. Thereafter, the dried samples were stored at 4 °C until subsequent DNA extraction.

For each plant sampled, shoots were dried at 37 °C for one week, and the dry weight was subsequently recorded. Roots were stored in 70% ethanol at 4 °C until root scanning. Root scans were taken using an Epson Dual Lens System Epson Perfection V800 Photo at 600 DPI in greyscale. RhizoVision Explorer version 2.0.3 (Seethepalli et al., 2021) was used to analyze the root scans. Scans were taken in “Broken roots” mode and at an image thresholding level of 175. Edge smoothing was enabled with a threshold of 3, and root pruning was enabled at a threshold of 10. Non-root objects below 2 mm^2 were removed. Total root length, average diameter, perimeter, volume, surface area, and branching frequency were calculated using RhizoVision (Seethepalli et al., 2021). After root scanning, the roots were dried at 37 °C for one week, and the dry weight was subsequently recorded.

Pot experiment set-up and sampling

High- and low-P field soil was collected from the Sawyers experimental field site at Rothamsted Research (Harpenden, UK). Soils from two historically low-P plots (last measured Olsen P = 7.1 mg/kg and 5.7 mg/kg in February 2022; A. Riche, personal communication, May 1, 2024) and two historically high-P plots (last measured Olsen P = 19.3 mg/kg and 18.6 mg/kg in February 2022; A. Riche, personal communication, May 1, 2024) were collected and mixed to create the low- and high-P potting soil, respectively. The soil was sieved through 4 mm mesh and mixed with washed sand (Horticultural Silver Sand, Melcourt, Tetbury, UK) in a 3:2 ratio (w/w) to improve drainage and root aeration. Samples of the soil-sand mixture were set aside at this point as low- and high-P bulk soil and stored at -80 °C. Characteristics of the low- and high-P soils are listed in Table S1. Two-liter pots (12 cm x 12 cm x 20 cm) were sterilized with Hortisept Pro (Conka, Nelson, UK), dried, and filled with the soil-sand mixture. Wild-type and mutant seeds were pre-germinated on moistened filter paper in the dark for three days before planting one seed per pot. Plants were grown in a climate chamber (Conviron CMP6010) under 16-hour days at 20 °C, 60% humidity, and light level 3, and 8-hour nights at 18 °C, 60% humidity and light level 0 for five weeks, at which the plants had reached booting stage (GS45 and GS47; Zadoks et al., 1974). Throughout growth, pots were rotated twice a week and watered according to weight approximately three times a week.

Plants were gently removed from the pots, and approximately half the root system was taken for rhizosphere and rhizoplane sampling as described in Guan et al. (2024). Rhizosphere and rhizoplane samples were stored at -80 °C until freeze-drying under vacuum at -70 °C; thereafter, the dried samples were stored at 4 °C until DNA extraction.

146 Shoots were dried at 37 °C for one week and subsequently the dry weight was recorded.
147 Roots were stored in 50% ethanol at 4 °C until AMF staining.

148 DNA extraction, quantification of bacterial P-cycling genes, and long-read Nanopore 16S
149 rRNA amplicon sequencing

150 DNA from up to 500 mg of freeze-dried rhizosphere from the field experiment and rhizosphere
151 and rhizoplane from the pot experiment was extracted using a FastPrep-24 5G beadbeating
152 system (MP Biomedicals, Irvine, CA, USA) at 6.0 m/s for 40 s and the FastDNA SPIN Kit for
153 soil (MP Biomedicals, Irvine, CA, USA) following the manufacturer's instructions. DNA quality
154 and quantity were tested using the NanoDrop ND-1000 spectrophotometer (Thermo Fisher
155 Scientific, Carlsbad, CA, USA) and a Qubit 2.0 Fluorometer (Thermo Fisher Scientific,
156 Carlsbad, CA, USA), respectively. DNA was diluted ten-fold to a quantity between 1 and 10
157 ng/µL.

158 Quantification of 16S rRNA genes and bacterial P-cycling genes (*bpp*, *phnK*, *phoD*, *phoX*, and
159 *pqqC*) in the samples was performed by qPCR using the AriaMx Real-Time PCR system
160 (Agilent Technologies, Santa Clara, CA, USA) following the methods described in Hao et al.
161 (2020). Primers are listed in Table S2. qPCR products were visualized on a 1% agarose gel
162 using GelRed (Sigma Aldrich, Denmark) to confirm amplification of the target gene. Standard
163 curves and negative controls were run in triplicate on each plate.

164 For long-read Nanopore amplicon sequencing of the 16S rRNA gene, PCR was used to
165 amplify 1050 bp of the 16S rRNA gene using primers 341F (5'- CCTACGGGNGGCWGCAG -
166 3') and 1391R (5'- GACGGGCGGTGWGTRCA -3') (Thijs et al., 2017) using Platinum SuperFi
167 II polymerase (Thermo Fischer Scientific, Waltham, USA). The ZymoBIOMICS Microbial
168 Community DNA Standard (Zymo Research, Irvine, CA, USA) was included as a sequencing
169 control. The PCR cycling conditions were as follows: an initial denaturation step of 98 °C for
170 30 s, followed by 30 cycles of denaturation at 98 °C for 10 s, annealing at 64 °C for 30 s, and
171 elongation at 72 °C for 45 s, and a final elongation at 72 °C for 5 m. PCR products were
172 visualized via electrophoresis on a 1% agarose gel before purification using AMPure XP beads
173 (Beckman Coulter Inc., Brea, CA, USA) at a 0.6 ratio. The sequencing library was prepared
174 using a native barcoding kit V14 (SQK-NBD114.96) and sequenced using a PromethION
175 R10.4.1 flow cell on the PromethION P2 Solo platform (Oxford Nanopore, UK). Adapter
176 trimming and basecalling was performed using Dorado version 0.7.0 using the super accurate
177 setting (github.com/nanoporetech/dorado).

178 Seqtk (github.com/lh3/seqtk) was used to discard reads below 1000 bp and above 1500 bp.
179 Amplicon sequences were extracted from between the primer sequences using
180 strip_degen_primer_deep (github.com/padbr/asat). NanoFilt version 2.8.0 (De Coster et al.,

181 2018) was used to discard amplicon sequences with an average quality score below 25.
182 Cutadapt version 3.5 (M. Martin, 2011) was used to truncate longer reads at 1010 bp. At this
183 point the remainder of the analysis was performed in R version 4.3.1 (R Core Team, 2023).
184 The reads were dereplicated to form amplicon sequence variants (ASVs) and assigned
185 taxonomy using dada2 version 1.22.0 (Callahan et al., 2016) with the SILVA database version
186 138.2 (Quast et al., 2013). The ASV table was transformed to a phyloseq object for
187 subsequent analysis using phyloseq version 1.44.0 (McMurdie & Holmes, 2013). ASVs
188 assigned to chloroplasts, mitochondria, and as non-bacterial were discarded before the ASVs
189 were agglomerated at the genus level while retaining non-classified reads. At this point, the
190 Zymo mock community was used to assess sequencing contamination. Ampvis2 version 2.8.1
191 (Andersen et al., 2018) was used to visualize bacterial community composition. A dissimilarity
192 matrix was calculated with rarefaction using avgdist() from the vegan package version 2.6-4
193 with default parameters (vegandevs.github.io/vegan). The rarefied dissimilarity matrix was
194 used to generate the principal coordinate analysis based on Bray-Curtis dissimilarities and to
195 run a PERMANOVA using adonis2() from vegan. Pairwise comparisons were made with the
196 package pairwiseAdonis version 0.4.1 (github.com/pmartinezarbizu/pairwiseAdonis). The
197 Shannon diversity index (alpha diversity) was calculated after rarefaction 100 times, as
198 proposed by Schloss, 2024. Briefly, the dataset was rarefied, and the Shannon diversity index
199 was subsequently calculated as the mean Shannon diversity index over 100 replicates.
200 Differentially abundant ASVs between the mutant and wild-type were generated using corncob
201 version 0.4.1 (B. D. Martin et al., 2020) with a false discovery rate of 0.05.

202 Raw reads are deposited in NCBI under BioProject PRJNA1308004.

203 P content of soil and shoots

204 High- and low-P bulk soil from the pot experiment was sent to NRM Cawood Scientific
205 (Bracknell, UK) for nutrient analysis. Soil pH, Olsens extractable P, and ammonium nitrate
206 extractable potassium (K) and magnesium (Mg) were measured. The bulk soil from the field
207 trial had a pH of 7.8 and an Olsens extractable P content of 12.8 mg/L (Table S1). The low-P
208 soil had an Olsens extractable P content of 10.0 mg/L, and the high-P was slightly higher at
209 13.7 mg/L (Table S1).

210 Dry shoot was homogenized and ground using a zirconium ball mill, and the P concentration
211 was determined using the dry ashing method of Saunders & Williams (1955) followed by the
212 molybdate-blue method (Murphy & Riley, 1962) using flow injection analysis (FIAstar 5000
213 analyzer, Foss, Hillerod, Denmark). Briefly, 100 mg samples were placed in acid-washed
214 crucibles and ashed in a muffle furnace at 550 °C for one hour. The ashes were mixed with
215 50 mL 0.5 M sulfuric acid and shaken overnight at room temperature. Extracts were filtered

216 through ashless filters (Whatman No. 42), and samples were diluted 10X before analysis. Two
217 blanks and one replicate of the standard reference material 1515 (NIST 1991) (Sigma Aldrich,
218 Denmark) were included in the analysis.

219 ### AMF quantification

220 Due to the small and fragile root system of the field-grown plants, relative qPCR was used to
221 quantify AMF colonization (Bodenhausen et al., 2021). DNA was extracted from the dried field-
222 grown roots using a FastPrep-24 5G beadbeating system (MP Biomedicals, Irvine, CA, USA)
223 at 6.0 m/s for 40 s and the FastDNA SPIN Kit (MP Biomedicals, Irvine, CA, USA) following the
224 manufacturer's instructions. DNA quality and quantity were tested as described above. DNA
225 was diluted ten-fold to a quantity between 1 and 10 ng/µL. AMF colonization was quantified
226 using the 18S rRNA gene fragment, amplified with the AMF-specific primers AMG1F (Hewins
227 et al., 2015) and AM1 (Helgason et al., 1998) (Table S2) on an AriaMx Real-Time PCR system
228 (Agilent Technologies, Santa Clara, CA, USA). The PCR program consisted of an initial
229 denaturation step of 15 min at 95 °C, followed by 45 cycles of denaturation at 95 °C for 15 s,
230 annealing at 62 °C for 30 s, and elongation at 72 °C for 20 s followed by a melting curve
231 analysis (from 65 to 95°C, with 0.5 °C steps holding for 5 s) (Bodenhausen et al., 2021). The
232 wheat gene encoding a heterogenous nuclear ribonucleoprotein Q, *hn-RNP-Q*, was amplified
233 with previously described primers (Qi et al., 2012) (Table S2) and was used to normalize the
234 AMF 18S rRNA gene signal. The PCR program consisted of an initial denaturation of 3 min at
235 95 °C, followed by 40 cycles of denaturation at 94 °C for 15 s, annealing at 58 °C for 15 s, and
236 elongation at 72 °C for 20 s followed by a melting curve analysis (from 61 to 95°C, with 0.5 °C
237 steps holding for 5 s). For both primer sets, each 20 µL qPCR reaction contained 10 µL 2X
238 Brilliant III Ultra-Fast SYBR Green qPCR Master Mix with Low ROX (Agilent Technologies,
239 Santa Clara, CA, USA), 0.4 µM each of forward and reverse primer, 1 mg/mL bovine serum
240 albumin (New England Bioabs, MA, USA), and 2 µL of template DNA. qPCR products were
241 visualized on a 1% agarose gel using GelRed (Sigma Aldrich, Denmark) to confirm
242 amplification of the target gene. Negative controls were run in triplicate for each primer pair.
243 Raw fluorescence data were imported to LinRegPCR (version 2021.2) (Ruijter et al., 2009) to
244 determine cycle number to threshold (Ct) and efficiency (*E*) using the default baseline
245 threshold from LinRegPCR. The normalized AMF 18S rRNA gene signal was normalized to
246 plant DNA as described by Bodenhausen et al. (2021).

247 In the pot experiment, AMF colonization was quantified via staining. From each plant,
248 approximately 40 sections of root measuring 1-2 cm in length were taken for AMF
249 quantification. Root samples were incubated in 2 mL microcentrifuge tubes containing 2 mL
250 10% KOH for 25 min at 90 ˚C. Subsequently, the KOH was removed, and the roots were
251 washed twice with distilled water. After washing, 2 mL 0.3 M HCl was added and incubated

for 30 min at room temperature. After removing the HCl, 2 mL 0.1% Trypan Blue stain was added and incubated for eight minutes at 90 ˚C. Roots were then washed twice with acidic glycerol (1:1 glycerol:0.3 M HCl v/v) and incubated with the last wash overnight at room temperature in the dark. No fewer than ten stained root sections per sample were mounted on microscope slides. Scoring for AMF presence and arbuscule formation was performed on 100 field of views per slide using a Leica DMLS microscope (Leica Microsystems, Wetzlar, Germany) under 200X magnification (Brundrett et al., 1996).

Statistical analysis

Data analysis was conducted in R version 4.3.1 (R Core Team, 2023), and all plots were created using ggplot2 version 3.5.1 (Wickham, 2016). Significance was defined as $p < 0.05$. Before linear model generation, the appropriate data transformation was identified using the Box-Cox transformation. All analyses of variance (ANOVAs) were performed using the car package version 3.0-5 (Fox & Weisberg, 2019) unless stated otherwise. All post-hoc pairwise comparisons were performed using the emmeans package version 1.10.4 (rvlenth.github.io/emmeans) with Tukey's HSD (Honestly Significant Difference) test. When applicable, the Benjamini & Hochberg method (Benjamini & Hochberg, 1995) was used to correct for multiple testing.

For field-grown plant parameters and AMF colonization, the Shapiro-Wilk test was used to check for normality between means. Welch Two Sample t-test was used to compare means for parametric groups, while a Wilcox test was used for non-parametric groups.

For pot-grown plant parameters and AMF colonization, a linear model was used to assess the effects of genotype and soil P status, followed by a two-way ANOVA. AMF colonization data was square root transformed. Shoot dry weight data was log transformed. Due to the presence of zeros in the arbuscule dataset, an aligned ranks transformation (ART) ANOVA was used as a non-parametric approach via the ARTool package version 0.11.1 (Kay et al., 2021).

All bacterial P-cycling qPCR data were log-transformed before analysis. For the field qPCR data, a linear model was used to assess the effects of sampling time point and sample source (root hair mutant, wild-type, or bulk soil) on gene relative abundance, followed by a two-way ANOVA. For the high- and low-P qPCR data, a linear model was used to assess the effects of genotype, soil condition, and compartment on gene relative abundance, followed by a three-way ANOVA.

Results

Root hair mutation affects belowground growth in the field only at the early seedling developmental stage

First, the roots of the mutant plants were visually assessed for root hair growth, confirming that the phenotype of arrested root hair elongation was maintained in a natural soil environment at GS11, GS12-GS13, and GS45 and GS47, and especially under low-P conditions (Figure S1).

To assess the effect of the *srh1* mutation on overall plant development under agricultural settings, ten growth parameters of the field-grown plants were measured. At two weeks post-sowing, the mutant had a smaller root system as defined by root dry weight, total root length, average diameter, perimeter, volume, surface area, and branching frequency (Figure 1). However, aboveground growth characteristics were unaffected (Figure 1A-B). At four weeks post-sowing, no difference was observed between the plants of the mutant and wild-type across all ten phenotypic parameters (Figure 1).

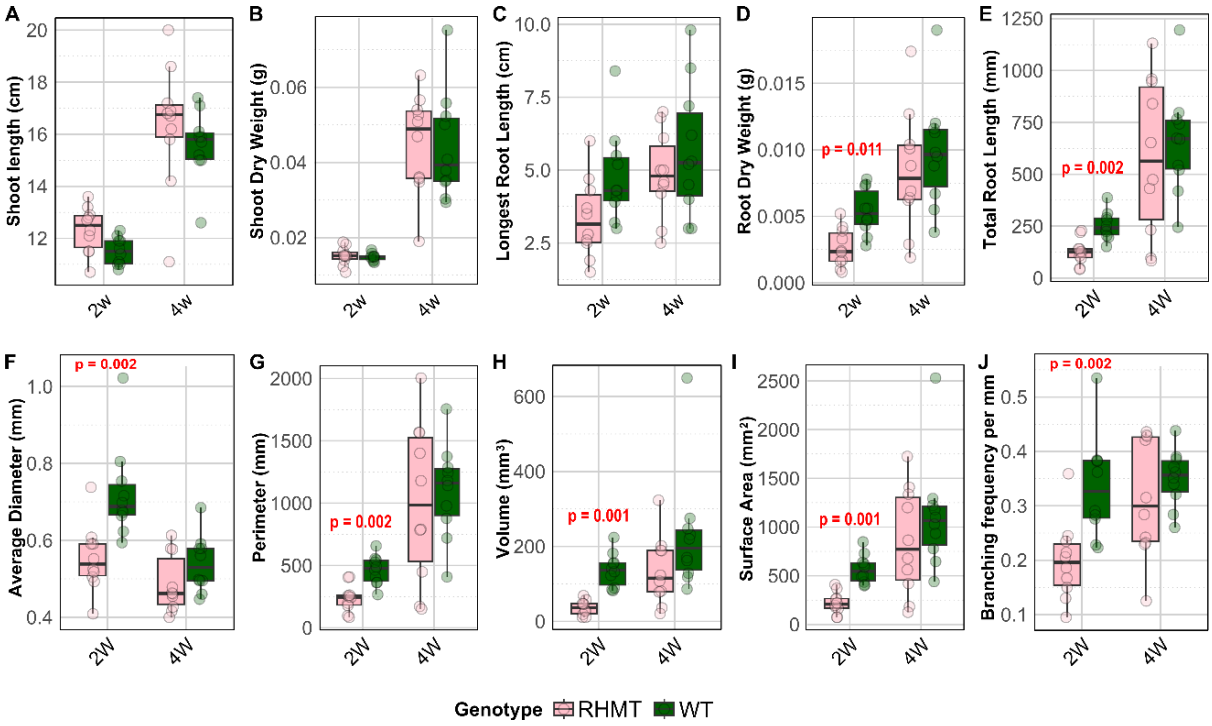

Figure 1. Root hair mutant (RHMT) and wild-type (WT) phenotypic parameters measured from field-grown plants, sampled at two (2W, n = 10) and four weeks (4W, n = 9) post-sowing. The boxplots display the median, the two hinges (25th and 75th percentile), and the upper and lower whiskers (extending to the largest and smallest values no further than 1.5 times the interquartile range). True data points are overlaid on the boxplots as filled circles. P-

304 values were calculated using the Wilcox test and adjusted for multiple testing using the
305 Benjamini & Hochberg method. Only p-values < 0.05 are shown.

306 ## The wheat root hair mutant shows temporal shift from bacterial P mineralization genes to AMF
307 colonization under field conditions

308 The ability of the root hair mutant to enrich its bacterial microbiome for P mobilization was
309 assessed using qPCR on DNA extracted from samples collected under field conditions across
310 early development. The relative abundance of all bacterial P-cycling genes analyzed, except
311 for *phoX,* was affected by sample source (root hair mutant, wild-type, or bulk soil) (two-way
312 ANOVA, $p < 0.05$). Neither sampling time point nor the interaction between sample source
313 and sampling time point influenced the relative abundance of the tested genes (two-way
314 ANOVA, $p > 0.05$). Because of this, pairwise comparisons were made only within each
315 sampling time point (Table 1).

316 At two weeks post-sowing, genes involved in bacterial organic P mineralization (*bpp* (beta-
317 propeller phytase), *phnK* (phosphonate degradation), and *phoD* (cytoplasmic phosphatase))
318 were enriched in the rhizosphere of wheat root hair mutants compared to wild-type (Table 1A).
319 The root hair mutant enriched these genes compared to the bulk soil, while the relative
320 abundance in the wild-type rhizosphere was similar to that of the bulk soil. The levels of *phoX*
321 (periplasmic phosphatase) and *pqqC* (pyrroloquinoline-quinone synthase) were equal
322 between the root hair mutant and wild-type. The relative abundance of the *pqqC* gene was
323 lower in the rhizosphere of both genotypes compared to the bulk soil.

324 At four weeks post-sowing, there was no enrichment of any of the targeted genes in the
325 rhizosphere of the root hair mutant compared to the wild-type (Table 1B). The relative
326 abundance of *bpp*, *phnK,* and *phoD* in the rhizosphere of the root hair mutant dropped to
327 match that of wild-type. Nevertheless, at this time, the relative abundance of the *bpp* gene
328 was still higher in the rhizosphere of both genotypes compared to the bulk soil. The relative
329 abundance of the *pqqC* gene continued to be lower in the rhizosphere of both genotypes
330 compared to the bulk soil at this time point.
331

Age	Genotype	*bpp*		*phnK*		*phoD*		*phoX*		*pqqC*	
2W	**RHMT**	1.14e-3 ± 7.05e-4	a	2.52e-1 ± 1.91e-1	a	2.77e-1 ± 2.56e-1	a	4.03e-2 ± 1.05e-2	a	3.75e-3 ± 2.83e-3	a
2W	**WT**	5.73e-4 ± 1.17e-4	b	1.21e-1 ± 2.32e-2	b	7.75e-2 ± 9.24e-3	b	4.28e-2 ± 7.21e-3	a	1.83e-3 ± 3.74e-4	a
2W	**Bulk Soil**	5.09e-4 ± 1.01e-4	b	1.10e-1 ± 2.92e-2	b	1.05e-1 ± 2.27e-2	ab	5.72e-2 ± 1.85e-2	a	6.42e-3 ± 2.00e-3	b
4W	**RHMT**	8.23e-4 ± 4.35e-4	a	1.82e-1 ± 1.32e-1	a	1.54e-1 ± 2.18e-1	a	4.50e-2 ± 1.16e-2	a	2.50e-3 ± 2.00e-3	a
4W	**WT**	6.31e-4 ± 1.63e-4	a	1.19e-1 ± 2.33e-2	ab	7.27e-2 ± 1.30e-2	a	4.69e-2 ± 1.50e-2	a	1.86e-3 ± 4.24e-4	a
4W	**Bulk Soil**	3.66e-4 ± 9.49e-5	b	8.31e-2 ± 1.05e-2	b	8.56e-2 ± 1.84e-2	a	4.81e-2 ± 1.28e-2	a	5.56e-3 ± 1.64e-3	b

Table 1. Relative abundance of bacterial P-cycling genes in root hair mutant (RHMT) and wild-type (WT) plants grown in the field and sampled at two weeks post-sowing (2W, n = 10) and four weeks post-sowing (4W, n = 9). Relative abundance was calculated by normalizing gene copy number to the 16S rRNA gene copy number in each sample measured by qPCR. Data are presented as the mean ± standard deviation. Bulk soil samples were from bare soil between the plots (no plant, n = 5). Means that share the same letter within each gene in each time point are not statistically different (Tukey adjusted post-hoc analysis, $p < 0.05$).

AMF colonization in the field was quantified by qPCR on DNA extracted from the roots of the field-grown plants. There was no effect of genotype nor interaction between genotype and age (two-way ANOVA, $p > 0.05$). However, there was an effect of age (two-way ANOVA, $p < 0.05$). Indeed, the plants sampled two weeks after sowing were colonized by AMF to a lesser extent than the plants sampled four weeks after sowing (Figure 2).

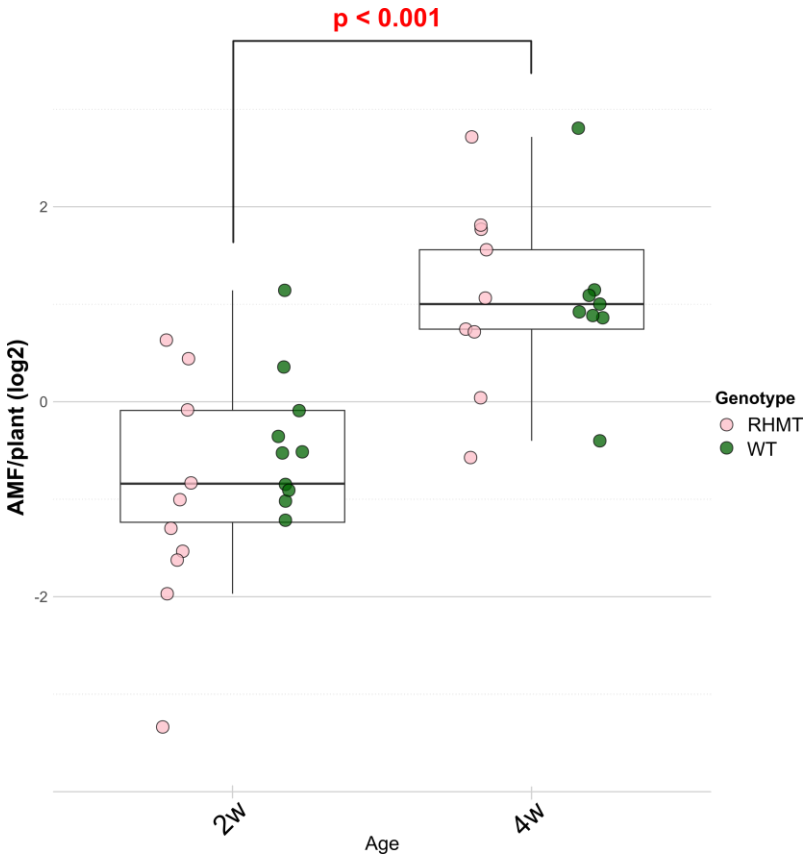

Figure 2. AMF signal quantified via qPCR and normalized to plant DNA in field-grown root hair mutant (RHMT) and wild-type (WT) plants two weeks (2W) and four weeks (4W) after sowing. The boxplots display the median, the two hinges (25th and 75th percentile), and the upper and lower whiskers (extending to the largest and smallest values no further than 1.5 times the interquartile range). True data points are overlaid on the boxplots as filled circles and colored by genotype. The mean of all 2W plants was compared to the mean of all 4W plants (Welch Two Sample t-test) after a two-way ANOVA determined no effect of genotype nor interaction between genotype and age ($p > 0.05$).

Soil P status impacts plant aboveground parameters at booting in the presence and absence of root hair elongation

To compare recruitment of bacterial P-cycling genes and AMF colonization at booting and under various levels of P fertilization, the root hair mutant and wild-type were grown in pots with soils from contrasting P management strategies and sampled at booting. To ensure the effect of the high- and low-P soils was realized, plant shoot growth and P content was measured at the time of sampling (Figure 3). Soil P status and genotype affected shoot length, shoot dry weight, and shoot P concentration (two-way ANOVA, $p < 0.05$), but there was no interaction between these two variables.

364 Regardless of genotype, plants in the low-P soils had lower shoot length (Figure 3A), shoot
365 biomass (Figure 3B) and shoot P concentration (Figure 3C) than in the high-P treatment.
366 Biomass in the low P soil was less than half of what was reached in the high P soil. In the
367 high-P soil, the wild-type performed better than the root hair mutant in terms of aboveground
368 growth, while the two genotypes were more equal under low-P conditions (Figure 3A-B). There
369 was no difference in P concentration between the two genotypes when grown in the same soil
370 (Figure 3C).

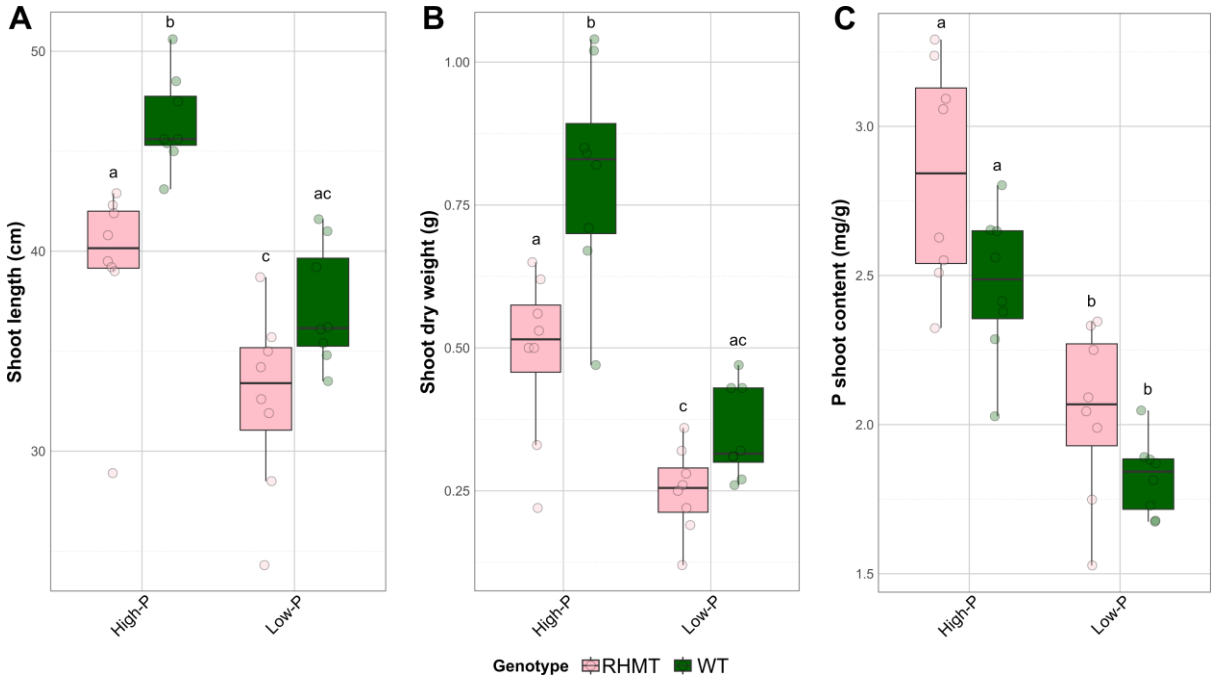

371

372 **Figure 3. Aboveground wheat growth parameters are affected by root hair mutation and**
373 **soil P status at booting.** Shoot length (A), shoot dry weight (B), and shoot P concentration
374 (C) for the root hair mutant (RHMT) and wild-type (WT) plants grown in high- and low-P soil.
375 The boxplots display the median, the two hinges (25th and 75th percentile), and the upper and
376 lower whiskers (extending to the largest and smallest values no further than 1.5 times the
377 interquartile range). True data points are overlaid on the boxplots as filled circles. Means that
378 share the same letter within each plot are not statistically different (Tukey adjusted post-hoc
379 analysis, $p < 0.05$).

380 At booting, the root hair mutant enhances AMF symbiosis but not bacterial P-cycling genes
381 under low- and high-P conditions

382 The relative abundances of the bacterial P-cycling genes were first assessed in the bulk high-
383 and low-P soils to determine the effect of soil fertilization history on the bacterial P-cycling
384 community. The relative abundances of all the targeted bacterial P-cycling genes were
385 different between high- and low-P bulk soils, with the high-P soil harboring a higher relative
386 abundance of all the tested bacterial P-cycling genes (Table 2A).

387 In the plant-associated soils, there was an effect of soil P status and rhizocompartment (i.e.
388 rhizoplane or rhizosphere) but not genotype on the relative abundances of *phoX*, *phoD*, and
389 *pqqC* (three-way ANOVA, $p < 0.05$). The relative abundance of *bpp* was only affected by
390 genotype (three-way ANOVA, $p < 0.05$). No factors had an impact on the relative abundance
391 of *phnk*. Regardless of rhizocompartment or soil P status, there was no enrichment of any of
392 the bacterial P-cycling genes in the root hair mutant compared to the wild-type (Table 2B).
393 Relative abundance in the rhizosphere and rhizoplane was only different between high- and
394 low-P conditions for the genes *phoD*, *phoX*, and *pqqC* (Table 2). The relative abundances of
395 the *bpp* and *phnk* genes in the rhizosphere and rhizoplane were equal between high- and low-
396 P soils (Table 2).

Compartment	Genotype	Condition	*bpp*		*phnK*		*phoD*		*phoX*		*pqqC*	
Plane	**RHMT**	**LowP**	2.16e-4 ± 1.76e-4	a	1.39e-1 ± 5.26e-2	a	2.79e-1 ± 5.95e-2	a	8.35e-4 ± 4.13e-4	a	2.29e-3 ± 8.94e-4	ab
Plane	**WT**	**LowP**	8.17e-4 ± 1.64e-3	a	1.56e-1 ± 5.46e-2	a	3.69e-1 ± 1.73e-1	a	8.68e-4 ± 4.00e-4	a	2.42e-3 ± 5.17e-4	ac
Plane	**RHMT**	**HighP**	2.57e-4 ± 6.97e-5	a	1.49e-1 ± 6.19e-2	a	4.89e-1 ± 1.27e-1	b	1.70e-3 ± 7.66e-4	b	3.40e-3 ± 1.22e-3	cd
Plane	**WT**	**HighP**	3.09e-4 ± 1.24e-4	a	1.52e-1 ± 5.27e-2	a	5.20e-1 ± 1.20e-1	b	1.71e-3 ± 7.52e-4	b	3.63e-3 ± 2.29e-3	bd
Sphere	**RHMT**	**LowP**	2.05e-4 ± 8.29e-5	a	1.49e-1 ± 5.06e-2	a	4.29e-2 ± 1.44e-2	a	1.46e-2 ± 6.55e-3	a	4.30e-3 ± 2.31e-3	ab
Sphere	**WT**	**LowP**	2.27e-4 ± 3.32e-5	a	1.47e-1 ± 4.13e-2	a	4.17e-2 ± 1.42e-2	a	1.32e-2 ± 4.36e-3	a	4.35e-3 ± 2.10e-3	ac
Sphere	**RHMT**	**HighP**	2.18e-4 ± 4.12e-5	a	1.45e-1 ± 4.30e-2	a	6.26e-2 ± 1.57e-2	b	3.24e-2 ± 1.06e-2	b	5.19e-3 ± 2.33e-3	cd
Sphere	**WT**	**HighP**	2.07e-4 ± 3.72e-5	a	1.81e-1 ± 3.40e-2	a	6.85e-2 ± 1.72e-2	b	4.02e-2 ± 1.42e-2	b	5.47e-3 ± 1.94e-3	bd
Bulk Soil		**LowP**	1.07e-4 ± 1.19e-5	b	7.22e-2 ± 9.72e-3	b	2.04e-1 ± 2.73e-2	b	2.58e-4 ± 5.95e-5	b	1.34e-3 ± 1.56e-4	b
Bulk Soil		**HighP**	2.31e-4 ± 6.75e-5	a	1.71e-1 ± 7.06e-2	a	4.66e-1 ± 1.49e-1	a	2.00e-3 ± 1.03e-3	a	2.68e-3 ± 1.02e-3	a

397 **Table 2. Relative abundance of bacterial P-cycling genes in root hair mutant (RHMT)**
398 **and wild-type (WT) plants grown under high-P and low-P soil conditions at booting in**
399 **the rhizoplane (plane, n = 8) and rhizosphere (sphere, n = 8), and in the bulk soil controls**
400 **(n = 5).** Relative abundance is calculated by normalizing the gene copy number to the 16S
401 rRNA gene copy number in each sample measured by qPCR. Data are presented as the mean

402 ± standard deviation. Means that share the same letter within each gene in each compartment
403 are not statistically different (Tukey adjusted post-hoc analysis, $p < 0.05$).

404 AMF staining revealed the extent of AMF colonization and arbuscule formation of the roots in
405 pot-grown plants at booting (Figure 4). Genotype, soil P status, and the interaction between
406 the two factors affected total AMF colonization (two-way ANOVA, $p < 0.05$). Likewise,
407 arbuscule formation was influenced by genotype and soil P status but not the interaction
408 between the two factors (ARTanova, $p < 0.05$). Under high-P, the root hair mutant harbored
409 more AMF than the wild-type, while at low-P, the colonization levels of the two genotypes were
410 equal (Figure 4A). With regards to arbuscule formation, the root hair mutant harbored a greater
411 percentage of arbuscules than the wild-type under both high- and low-P conditions (Figure
412 4B). Both genotypes displayed greater arbuscular formation under low-P than high-P (Figure
413 4B).

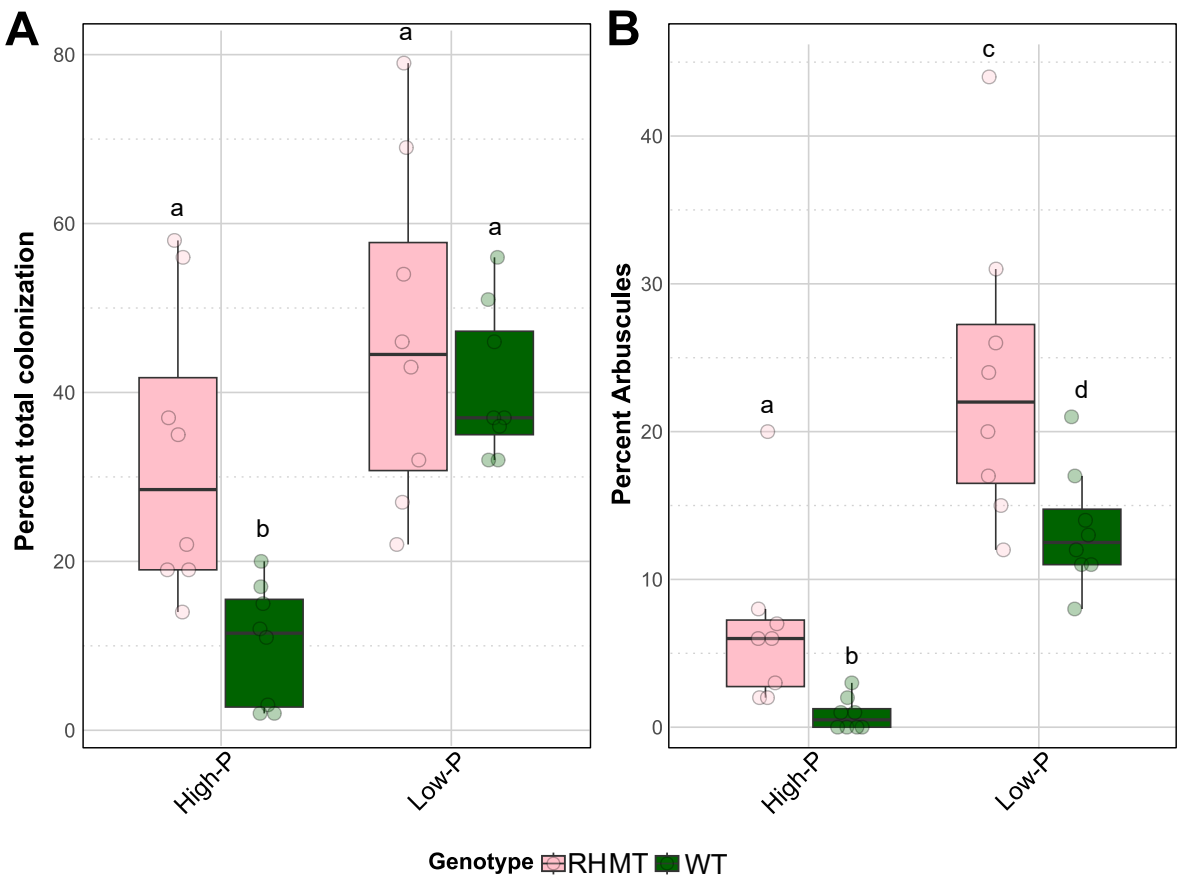

414

415 **Figure 4. Total arbuscular mycorrhizal fungi (AMF) colonization (A) and arbuscule**
416 **formation (B) in wild-type (WT) and root hair mutant (RHMT) plants grown in pots under**
417 **high- and low-P conditions at booting.** The boxplots display the median, the two hinges
418 (25th and 75th percentile), and the upper and lower whiskers (extending to the largest and
419 smallest values no further than 1.5 times the interquartile range). True data points are overlaid

on the boxplots as filled circles. Means that share the same letter within each plot are not statistically different (Tukey adjusted post-hoc analysis, $p < 0.05$).

Rhizosphere bacterial community composition is affected by the lack of root hair elongation in older plants

To reveal the rhizosphere bacterial community taxonomic composition, long-read 16S rRNA amplicon sequencing was performed on the rhizosphere of field-and pot-grown plants. After filtering, 1,264,834 reads were retained across the two sequencing datasets. Across the field-grown plants, 677,509 reads were assigned to 1,337 ASVs, and 80.2% of ASVs were identified at the genus level. The median reads per sample was 14,621. Across the pot-grown plants, 587,325 reads were assigned to 1,263 ASVs, with 80.5% of the ASVs identified at the genus level. The median reads per sample was 14,519.5.

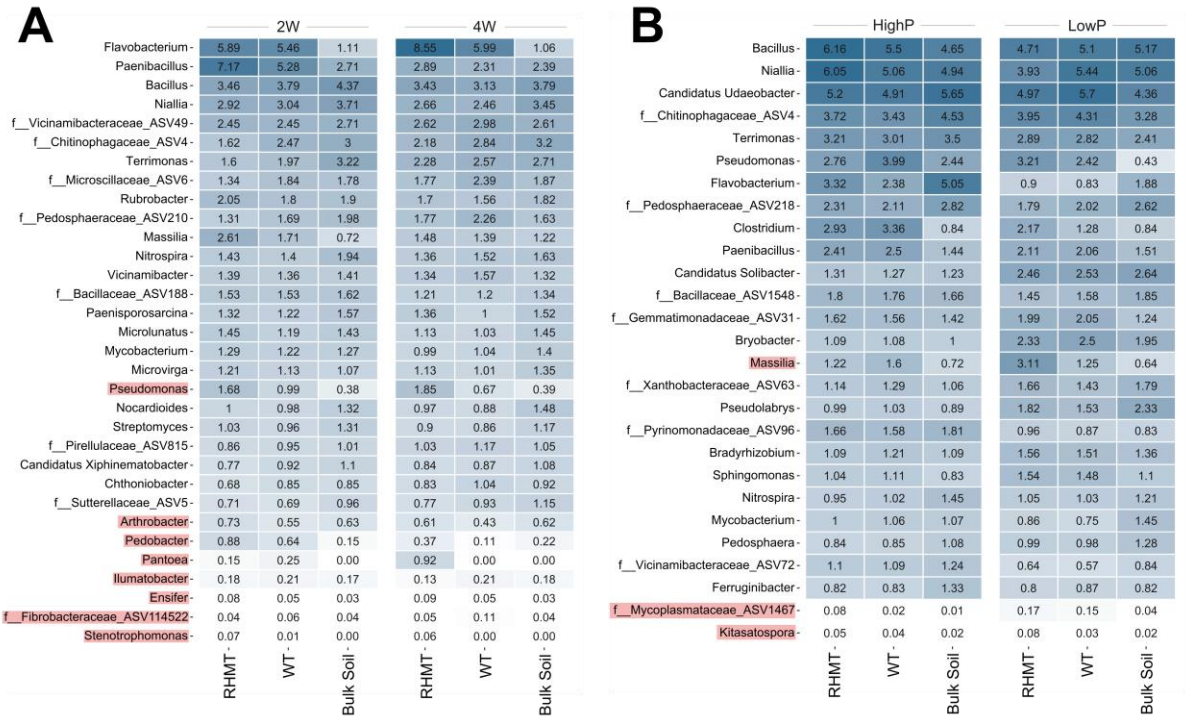

Figure 5. The relative abundance of the top 25 bacterial genera, plus genera identified as differentially abundant between the root hair mutant (RHMT) and wild-type (WT), highlighted in red, in the rhizosphere of field-grown plants (A) and pot-grown plants (B) compared to bulk soil. The heatmap displays the mean relative abundances of the samples within a treatment: two weeks post-sowing (2W) mutant (n = 10) and wild-type (n = 9); four weeks post-sowing (4W) mutant (n = 10) and wild-type (n = 8); booting in high-P soil (HighP) mutant (n = 8) and wild-type (n = 8); booting in low-P soil (LowP) mutant (n = 6) and wild-type (n = 6). Bulk soil samples were taken from unplanted soil (n = 5).

440 For the field-grown plants, long-read 16S rRNA amplicon sequencing identified an impact of
441 genotype (PERMANOVA, $p = 0.020$, $R^2 = 0.06$) and age (PERMANOVA, $p = 0.001$, $R^2 = 0.11$)
442 on the bacterial community in the rhizosphere (Figure S2A). Pairwise comparisons between
443 the genotypes at two- and four-weeks post-sowing revealed that only the microbiome of four-
444 week-old plants were different ($p = 0.031$). Indeed, there were no bacterial genera that were
445 enriched in one genotype or the other at two weeks post-sowing. On the other hand, at four
446 weeks post-sowing, *Ilumatobacter* and an unidentified genus of the Fibrobacteraceae family
447 were enriched in wild-type plants, while *Arthrobacter, Ensifer*, *Pseudomonas*,
448 *Stenotrophomonas*, *Pedobacter*, and *Pantoea* were enriched in the mutant (Figure 5A, Figure
449 S2B). Alpha diversity of the microbiome was not different between the wild-type and the
450 mutant at either sampling time point (Figure S2C).

451 In the pot-grown plants, soil P status (PERMANOVA, $p = 0.001$, $R^2 = 0.36$) and the interaction
452 between genotype and soil P status (PERMANOVA, $p = 0.014$, $R^2 = 0.07$) impacted the
453 bacterial microbiome in the rhizosphere (Figure S2D). Pairwise comparisons revealed that
454 under high P conditions and low P conditions, the rhizosphere microbiome of the two
455 genotypes were different ($p = 0.036$ and $= 0.029$, respectively). Under high P soil conditions,
456 an unknown genus of the Mycoplasmataceae family was enriched in the mutant (Figure 5B,
457 Figure S2E). Under low P conditions, the genera *Massilia* and *Kitasatospora* were enriched in
458 the mutant (Figure 5B, Figure S2E). There were no taxa differentially enriched in the wild-type
459 in either soil. Alpha diversity of the microbiome was not different between the wild-type and
460 the mutant in either high P or low P conditions (Figure S2F).

461 Discussion

462 The potential of the plant to utilize its bacterial and fungal microbiome for P nutrition has yet
463 to be fully understood. In this work, we used a novel root hair mutant in wheat to reduce the
464 dominance of root hair plasticity response in P uptake and highlight the ability of wheat to
465 exploit the soil microbiome for P nutrition. We tested the hypothesis that the root hair mutant
466 would boost recruitment of P-cycling bacteria and AMF to compensate for the loss of root hair
467 elongation, which was maintained in the root hair mutant at each growth stage and under all
468 conditions.

469 Initial screenings demonstrated the stunting effect of the *srh1* mutation on early root
470 development, which can in turn influence the rhizosphere microbiome (Saleem et al., 2018;
471 Herms et al., 2022). In preliminary studies, primary and total root length was shown to be
472 longer in the mutant compared to wild-type when grown in agar (Tsang, Thomelin, et al.,
473 2024). Our results indicate that the root hair mutant grown in soil is delayed in root system
474 development, which is mirrored by diminished aboveground biomass at booting (GS45 and

475 GS47). Reduced root growth and development is typical in hairless soil-grown crops due to
476 the importance of root hairs in overall crop development (Haling et al., 2013; Ma et al., 2020;
477 Suzuki et al., 2003).

478 We demonstrate that the loss of root hairs affects the P-cycling bacterial community during
479 early wheat development under field conditions. We establish support for our hypothesis that
480 the root hair mutant can enrich bacterial P mineralization genes in the rhizosphere under field
481 conditions. Relative abundance of the P solubilization-related gene *pqqC*, the co-factor for
482 gluconic acid production (An & Moe, 2016), was no different between the root hair mutant and
483 wild-type. Since plants normally rely on root hairs to mobilize organic P into orthophosphate
484 anions (Gahoonia et al., 2001; Ma et al., 2020; Richardson et al., 2011), the specific
485 enrichment of bacterial organic P mineralization genes in the root hair mutant suggests a
486 bacterial route for organic P acquisition to compensate for the loss of root hairs. Indeed,
487 bacteria fed by plant root exudates play a significant role in organic P mineralization in the soil
488 (Wang et al., 2025), indicating a potential relationship between microbial function and plant
489 needs. While we cannot rule out competition for P between bacteria and the plant (Raymond
490 et al., 2021), niche-filling in the rhizosphere of the root hair mutant would arguably enrich all
491 P-bacterial cycling genes, not selectively mineralization, as competitors for P in the soil
492 proliferate in the carbon-rich rhizosphere.

493 However, bacterial P mineralization genes were only enriched in the root hair mutant at two
494 weeks post-sowing. Sampling two weeks later at GS12-GS13 revealed that the relative
495 abundance of organic P mineralization genes in the root hair mutant rhizosphere dropped to
496 match that of the wild-type.

497 While P uptake in the first weeks of growth plays a role in seedling vigor (Yi et al., 2023), the
498 rate of P uptake in wheat reaches its maximum during booting (Jones et al., 2024). Thus,
499 regardless of the loss of enrichment for bacterial P cycling genes in the mutant at four weeks
500 post-sowing (GS12-GS13) in the field, we hypothesized to see enrichment of P-cycling genes
501 in the mutant at booting, exacerbated further by the inclusion of a low-P managed soil.
502 However, this hypothesis was not supported; at booting (GS45 and GS47) in the pots, relative
503 abundances of all bacterial P-cycling genes were equal between the mutant and wild-type.
504 Soil P affected bacterial P-cycling gene relative abundance regardless of root hair status.
505 Previously, high P inputs have been shown to correlate with the increased ability of bacteria
506 to interact with soil P (Dai et al., 2020; Xiao et al., 2022). The enrichment of the *phoD* gene in
507 the rhizosphere in response to soil fertilization supports a similar response previously reported
508 (Liu et al., 2021). Nevertheless, since two different soils were used in the field and pot
509 experiments, direct comparisons of the bacterial P mineralization response to the root hair

510 mutant between these experiments must be carefully interpreted. Ideally, measurements of
511 organic P in the field versus the pots would provide further insights into how organic P
512 conditions in the soil may influence the responsiveness of organic P mineralization genes in
513 the rhizosphere of the root hair mutant.

514 There was a tangible effect of the loss of root hairs on bacterial community composition, but
515 we could not see meaningful links between the long-read 16S rRNA amplicon sequencing and
516 the bacterial qPCR results. That is, only older plants showed a compositional difference
517 between the mutant and the wild-type, despite functional differences appearing in the
518 youngest plants. This was likely because 16S rRNA sequences, even full-length, are poor
519 proxies for functional capabilities (Jaspers & Overmann, 2004), a statement we have also
520 found to be true in wheat rhizosphere *Pseudomonas* isolates (Herms et al., 2025). Thus,
521 taxonomic profiling is not an appropriate representation of P-cycling capabilities, and we
522 therefore prioritize the results of the qPCR analyses for interpretation of P-cycling.
523 Nevertheless, we still contribute evidence for the role of root hairs in shaping the bacterial
524 community in the wheat rhizosphere, especially as the plants matured, as found in barley and
525 maize (Quattrone et al., 2024; Robertson-Albertyn et al., 2017). This can be attributed to the
526 loss of unique colonization niches (Buddrus-Schiemann et al., 2010; Mousa et al., 2016) or
527 altered root exudate profiles compared to their wild-type background (Galloway et al., 2022;
528 Lohse et al., 2023; Sasse et al., 2018). Analysis of the root exudates of the wheat root hair
529 mutant, while out of scope in this work, could help clarify this dysbiosis.

530 The drop in bacterial P mineralization genes at GS12-GS13 in the root hair mutant coincided
531 with a marked increase in AMF colonization levels across the plants from GS11 to GS12-
532 GS13. Typically, it takes growth equal to GS12 to identify AMF colonization in field-grown
533 wheat (Marrassini et al., 2024), because the root system needs to be fully developed before
534 the symbiosis can be initiated (Werner & Kiers, 2015). Root growth of the mutant matched that
535 of the wild-type at this time, potentially indicating a readiness for AMF colonization or,
536 alternatively, representing a direct root response to AMF colonization (Zhu et al., 2025).
537 Collectively, these findings indicate a temporal shift from enrichment of bacterial P-cycling to
538 dominance of the AMF symbiosis. In support of this, we observed no enrichment of bacterial
539 P-cycling genes in the root hair mutant at booting (GS45 and GS47), when P uptake is highest
540 in wheat (Jones et al., 2024), nor when we induced additional P stress via cultivation in low-P
541 soil. At GS45 and GS47, the roots were also heavily colonized by AMF. However, since this
542 work took place across two different soils, the AMF communities, colonization potential, and
543 responsiveness may be different between the field and the pots (Jansa et al., 2014) and direct
544 parallels between the experiments must be interpreted with caution. Taken together, our
545 results suggest that before the AMF symbiosis is fully dominant, wheat can recruit and rely on

546 bacterial P mineralization to meet their P needs and then release these bacterial players once
547 the AMF symbiosis is developed.

548 It is well known that plants enrich AMF colonization when grown under limited P (Kumar et al.,
549 2019; Zhou et al., 2022; Wang et al., 2025). Root hair mutant plants also display a similar
550 response of increased AMF colonization, likely as a compensatory mechanism for nutrient
551 uptake in the absence of root hairs (Jakobsen et al., 2005; Kumar et al., 2019; Ma et al., 2020).
552 Our results add further evidence to the conserved ability of cereal crops to increase AMF
553 recruitment when root hair development is inhibited. Notably, we saw higher AMF
554 arbuscularisation in the root hair mutant, regardless of soil P status. Arbuscules are the
555 specialized mycorrhizal structures that facilitate mineral nutrient translocation from fungus to
556 plant (Smith & Smith, 2011). This result indicates not only enhanced colonization by AMF, but
557 also a reliance of the root hair mutant on AMF for mineral P uptake. This gives further credibility
558 to our claim that in the root hair mutant, AMF replace P mineralizing bacteria. Ideally,
559 quantifying P stress across developmental stages when the plant is grown only with P-cycling
560 bacteria or only with AMF would solidify the importance of these microorganisms in wheat P
561 uptake.

562 Our results also indicate that AMF may play a greater role than root hairs in wheat performance
563 under low-P conditions. In the field and in high-P soil, the root hair mutant had stunted growth
564 compared to the wild-type, as expected (Haling et al., 2013; Ma et al., 2020; Suzuki et al.,
565 2003). However, under low-P conditions, there was no difference in biomass between the two
566 genotypes at booting. The combination of the loss of root hairs with low-P soil should increase
567 the stress of the plant (Gahoonia et al., 2001), but the root hair mutant coped relatively well.
568 There was even a non-significant trend of the mutant having higher shoot P concentration than
569 the wild-type under low-P conditions. Under low-P, the root hair mutant boasts high AMF
570 colonization and increased arbuscule formation. Taken together, these results suggest the
571 greater influence of AMF compared to root hairs in wheat P nutrition. This was the same
572 conclusion previously made in maize, where inoculation of a root hairless mutant with AMF in
573 low-P conditions resulted in better performance than the wild-type grown under the same
574 conditions (Ma et al., 2020).

575 Despite decades of research, successfully manipulating the rhizosphere microbiome for
576 improved crop nutrition remains limited. Our results shed light on how hairless wheat roots
577 can rely on their bacterial and fungal partners for P nutrition. Collectively, this work can be
578 used to guide improvements of the microbial P uptake mechanisms in wheat. By considering
579 the natural ecology in the rhizosphere of the root hair mutant, we recommend focusing on

580 bacterial interactions only during the early stages of wheat development and otherwise
581 prioritizing the AMF symbiosis throughout wheat growth.

582 Acknowledgements

583 The authors thank Andrew Riche (Rothamsted Research, Harpenden, UK) for access to the
584 high- and low-P managed soils. This study was funded by the Novo Nordisk Foundation (Grant
585 number: NNF19SA0059360) and the Biotechnology and Biological Sciences Research
586 Council (BBSRC) as part of the Collaborative Training Program for Sustainable Agricultural
587 Innovation (CTP-SAI) (grant BB/W009439/1) in partnership with The Morley Agricultural
588 Foundation (TMAF). We thank Stephen Rawsthorne (TMAF) and Jonathan Atkinson
589 (University of Nottingham, UK) for their inputs into IT's PhD. Further support to CHH was
590 provided by the European Molecular Biology Organization (EMBO) and the Monogram
591 Network.

592 Competing interests

593 The authors declare no competing interests that may influence the outcome of this work.

594 Author Contributions

595 Courtney Horn Herms: design of the research; performance of the research; data analysis,
596 collection, or interpretation; writing the manuscript. Ian Tsang: data analysis, collection, or
597 interpretation; writing the manuscript. Frederik Bak: data analysis, collection, or
598 interpretation; writing the manuscript. Klara Gunnarsen: data analysis, performance of the
599 research; collection, or interpretation; writing the manuscript. Magdalena Hasenzagl: data
600 analysis, collection, or interpretation; writing the manuscript. Amaru Miranda Djurhuus: data
601 analysis, performance of the research; collection, or interpretation; writing the manuscript.
602 Tom Thirkell: data analysis, collection, or interpretation; writing the manuscript. Eric Ober:
603 design of the research; data analysis, collection, or interpretation; writing the manuscript.
604 Fiona Leigh: design of the research; data analysis, collection, or interpretation; writing the
605 manuscript. James Cockram: design of the research; data analysis, collection, or
606 interpretation; writing the manuscript. Mette Haubjerg Nicolaisen: design of the research;
607 data analysis, collection, or interpretation; writing the manuscript.

608 Data Availability

609 16S rRNA amplicon sequence data is publicly available on NCBI under BioProject
610 PRJNA1308004. Raw data is presented in the figures when applicable. All other raw data is
611 available upon request.

References

An, R., & Moe, L. A. (2016). Regulation of Pyrroloquinoline Quinone-Dependent Glucose Dehydrogenase Activity in the Model Rhizosphere-Dwelling Bacterium Pseudomonas putida KT2440. *Applied and Environmental Microbiology*, *82*(16), 4955–4964. https://doi.org/10.1128/AEM.00813-16

Andersen, K. S., Kirkegaard, R. H., Karst, S. M., & Albertsen, M. (2018). ampvis2: An R package to analyse and visualise 16S rRNA amplicon data. *bioRxiv*. https://doi.org/10.1101/299537

Azaroual, S. E., Hazzoumi, Z., Mernissi, N. E., Aasfar, A., Meftah Kadmiri, I., & Bouizgarne, B. (2020). Role of Inorganic Phosphate Solubilizing Bacilli Isolated from Moroccan Phosphate Rock Mine and Rhizosphere Soils in Wheat (Triticum aestivum L) Phosphorus Uptake. *Current Microbiology*, *77*(9), 2391–2404. https://doi.org/10.1007/s00284-020-02046-8

Bates, T. R., & Lynch, J. P. (1996). Stimulation of root hair elongation in Arabidopsis thaliana by low phosphorus availability. *Plant, Cell & Environment*, *19*(5), 529–538. https://doi.org/10.1111/j.1365-3040.1996.tb00386.x

Benjamini, Y., & Hochberg, Y. (1995). Controlling the False Discovery Rate: A Practical and Powerful Approach to Multiple Testing. *Journal of the Royal Statistical Society: Series B (Methodological)*, *57*(1), 289–300. https://doi.org/10.1111/j.2517-6161.1995.tb02031.x

Bergkemper, F., Schöler, A., Engel, M., Lang, F., Krüger, J., Schloter, M., & Schulz, S. (2016). Phosphorus depletion in forest soils shapes bacterial communities towards phosphorus recycling systems. *Environmental Microbiology*, *18*(6), 1988–2000. https://doi.org/10.1111/1462-2920.13188

Bodenhausen, N., Deslandes-Hérold, G., Waelchli, J., Held, A., van der Heijden, M. G. A., & Schlaeppi, K. (2021). Relative qPCR to quantify colonization of plant roots by arbuscular mycorrhizal fungi. *Mycorrhiza*, *31*(2), 137–148. https://doi.org/10.1007/s00572-020-01014-1

Brown, L. K., George, T. S., Thompson, J. A., Wright, G., Lyon, J., Dupuy, L., Hubbard, S. F., & White, P. J. (2012). What are the implications of variation in root hair length on tolerance to phosphorus deficiency in combination with water stress in barley (Hordeum vulgare)? *Annals of Botany*, *110*(2), 319–328. https://doi.org/10.1093/aob/mcs085

Brundrett, M., Bougher, N., Dell, B., Grove, T., & Malajczuk, N. (1996). *Working with Mycorrhizas in Forestry and Agriculture*. https://doi.org/10.13140/2.1.4880.5444

Buddrus-Schiemann, K., Schmid, M., Schreiner, K., Welzl, G., & Hartmann, A. (2010). Root Colonization by Pseudomonas sp. DSMZ 13134 and Impact on the Indigenous Rhizosphere Bacterial Community of Barley. *Microbial Ecology*, *60*(2), 381–393. https://doi.org/10.1007/s00248-010-9720-8

Callahan, B. J., McMurdie, P. J., Rosen, M. J., Han, A. W., Johnson, A. J. A., & Holmes, S. P. (2016). DADA2: High-resolution sample inference from Illumina amplicon data. *Nature Methods*, *13*(7), 581–583. https://doi.org/10.1038/nmeth.3869

Dai, Z., Liu, G., Chen, H., Chen, C., Wang, J., Ai, S., Wei, D., Li, D., Ma, B., Tang, C., Brookes, P. C., & Xu, J. (2020). Long-term nutrient inputs shift soil microbial functional profiles of phosphorus cycling in diverse agroecosystems. *The ISME Journal*, *14*(3), 757–770. https://doi.org/10.1038/s41396-019-0567-9

De Coster, W., D'Hert, S., Schultz, D. T., Cruts, M., & Van Broeckhoven, C. (2018). NanoPack: Visualizing and processing long-read sequencing data. *Bioinformatics*, *34*(15), 2666–2669. https://doi.org/10.1093/bioinformatics/bty149

Fox, J., & Weisberg, S. (2019). *An R Companion to Applied Regression* (Third). Sage. https://www.john-fox.ca/Companion/

Gahoonia, T. S., Nielsen, N. E., Joshi, P. A., & Jahoor, A. (2001). A root hairless barley mutant for elucidating genetic of root hairs and phosphorus uptake. *Plant and Soil*, *235*(2), 211–219. https://doi.org/10.1023/A:1011993322286

Galloway, A. F., Akhtar, J., Burak, E., Marcus, S. E., Field, K. J., Dodd, I. C., & Knox, P. (2022). Altered properties and structures of root exudate polysaccharides in a root hairless mutant of barley. *Plant Physiology*, *190*(2), 1214–1227. https://doi.org/10.1093/plphys/kiac341

Ge, A.-H., & Wang, E. (2025). Exploring the plant microbiome: A pathway to climate-smart crops. *Cell*, *188*(6), 1469–1485. https://doi.org/10.1016/j.cell.2025.01.035

Guan, Y., Bak, F., Hennessy, R. C., Horn Herms, C., Elberg, C. L., Dresbøll, D. B., Winding, A., Sapkota, R., & Nicolaisen, M. H. (2024). The potential of Pseudomonas fluorescens SBW25 to produce viscosin enhances wheat root colonization and shapes root-associated microbial communities in a plant genotype-dependent manner in soil systems. *mSphere*, *9*(7), e00294-24. https://doi.org/10.1128/msphere.00294-24

Haling, R. E., Brown, L. K., Bengough, A. G., Young, I. M., Hallett, P. D., White, P. J., & George, T. S. (2013). Root hairs improve root penetration, root–soil contact, and phosphorus acquisition in soils of different strength. *Journal of Experimental Botany*, *64*(12), 3711–3721. https://doi.org/10.1093/jxb/ert200

Hao, X., Zhu, Y.-G., Nybroe, O., & Nicolaisen, M. H. (2020). The Composition and Phosphorus Cycling Potential of Bacterial Communities Associated With Hyphae of Penicillium in Soil Are Strongly Affected by Soil Origin. *Frontiers in Microbiology*, *10*. https://doi.org/10.3389/fmicb.2019.02951

Helgason, T., Daniell, T. J., Husband, R., Fitter, A. H., & Young, J. P. W. (1998). Ploughing up the wood-wide web? *Nature*, *394*(6692), 431–431. https://doi.org/10.1038/28764

Herms, C. H., Hennessy, R. C., Bak, F., Dresbøll, D. B., & Nicolaisen, M. H. (2022). Back to our roots: Exploring the role of root morphology as a mediator of beneficial plant–microbe interactions. *Environmental Microbiology*, *00*. https://doi.org/10.1111/1462-2920.15926

Herms, C. H., Hennessy, R. C., Bak, F., Guan, Y., Browne, P. D., Nielsen, T. K., Hansen, L. H., Dresbøll, D. B., & Nicolaisen, M. H. (2025). *Pseudomonas* taxonomic and functional microdiversity in the wheat rhizosphere is cultivar-dependent and links to disease resistance profile and root diameter. *Applied Soil Ecology*, *211*, 106116. https://doi.org/10.1016/j.apsoil.2025.106116

Hewins, C. R., Carrino-Kyker, S. R., & Burke, D. J. (2015). Seasonal variation in mycorrhizal fungi colonizing roots of Allium tricoccum (wild leek) in a mature mixed hardwood forest. *Mycorrhiza*, *25*(6), 469–483. https://doi.org/10.1007/s00572-015-0628-5

Jakobsen, I., Chen, B., Munkvold, L., Lundsgaard, T., & Zhu, Y.-G. (2005). Contrasting phosphate acquisition of mycorrhizal fungi with that of root hairs using the root hairless barley mutant. *Plant, Cell & Environment*, *28*(7), 928–938. https://doi.org/10.1111/j.1365-3040.2005.01345.x

Jansa, J., Erb, A., Oberholzer, H.-R., Šmilauer, P., & Egli, S. (2014). Soil and geography are more important determinants of indigenous arbuscular mycorrhizal communities than management practices in Swiss agricultural soils. *Molecular Ecology*, *23*(8), 2118–2135. https://doi.org/10.1111/mec.12706

Jaspers, E., & Overmann, J. (2004). Ecological Significance of Microdiversity: Identical 16S rRNA Gene Sequences Can Be Found in Bacteria with Highly Divergent Genomes and Ecophysiologies. *Applied and Environmental Microbiology*, *70*(8), 4831–4839. https://doi.org/10.1128/AEM.70.8.4831-4839.2004

Jensen, C. N. G., Pang, J. K. Y., Gottardi, M., Kračun, S. K., Svendsen, B. A., Nielsen, K. F., Kovács, Á. T., Moelbak, L., Fimognari, L., Husted, S., & Schulz, A. (2024). Bacillus subtilis promotes plant phosphorus (P) acquisition through P solubilization and stimulation of root and root hair growth. *Physiologia Plantarum*, *176*(3), e14338. https://doi.org/10.1111/ppl.14338

Jones, C., Olson-Rutz, K., & Dinkins, C. (2024, March). *Nutrient Uptake Timing by Crops to Assist with Fertilizing Decisions*. Montana State University Extension.

Kay, M., Elkin, L. A., Higgins, J. J., & Wobbrock, J. O. (2021). *ARTool: Aligned Rank Transform for Nonparametric Factorial ANOVAs*. https://doi.org/10.5281/zenodo.594511

Krasileva, K. V., Vasquez-Gross, H. A., Howell, T., Bailey, P., Paraiso, F., Clissold, L., Simmonds, J., Ramirez-Gonzalez, R. H., Wang, X., Borrill, P., Fosker, C., Ayling, S., Phillips, A. L., Uauy, C., & Dubcovsky, J. (2017). Uncovering hidden variation in polyploid wheat. *Proceedings of the National Academy of Sciences*, *114*(6), E913–E921. https://doi.org/10.1073/pnas.1619268114

Kumar, A., Shahbaz, M., Koirala, M., Blagodatskaya, E., Seidel, S. J., Kuzyakov, Y., & Pausch, J. (2019). Root trait plasticity and plant nutrient acquisition in phosphorus limited soil. *Journal of Plant Nutrition and Soil Science*, *182*(6), 945–952. https://doi.org/10.1002/jpln.201900322

Liu, W., Ling, N., Luo, G., Guo, J., Zhu, C., Xu, Q., Liu, M., Shen, Q., & Guo, S. (2021). Active *phoD*-harboring bacteria are enriched by long-term organic fertilization. *Soil Biology and Biochemistry*, *152*, 108071. https://doi.org/10.1016/j.soilbio.2020.108071

Lohse, M., Santangeli, M., Steininger-Mairinger, T., Oburger, E., Reemtsma, T., Lechtenfeld, O. J., & Hann, S. (2023). The effect of root hairs on exudate composition: A comparative non-targeted metabolomics approach. *Analytical and Bioanalytical Chemistry*, *415*(5), 823–840. https://doi.org/10.1007/s00216-022-04475-9

Ma, X., Li, X., & Ludewig, U. (2020). Arbuscular mycorrhizal colonization outcompetes root hairs in maize under low phosphorus availability. *Annals of Botany*, *127*(1), 155. https://doi.org/10.1093/aob/mcaa159

Marrassini, V., Ercoli, L., Piazza, G., & Pellegrino, E. (2024). Plant genotype and inoculation with indigenous arbuscular mycorrhizal (AM) fungi modulate wheat productivity and quality of processed products through changes in the frequency of root AM fungal taxa. *Field Crops Research*, *315*, 109456. https://doi.org/10.1016/j.fcr.2024.109456

Martin, B. D., Witten, D., & Willis, A. D. (2020). Modeling microbial abundances and dysbiosis with beta-binomial regression. *The Annals of Applied Statistics*, *14*(1), 94–115. https://doi.org/10.1214/19-AOAS1283

Martin, M. (2011). Cutadapt removes adapter sequences from high-throughput sequencing reads. *EMBnet.Journal*, *17*(1), Article 1. https://doi.org/10.14806/ej.17.1.200

McMurdie, P. J., & Holmes, S. (2013). phyloseq: An R Package for Reproducible Interactive Analysis and Graphics of Microbiome Census Data. *PLOS ONE*, *8*(4), e61217. https://doi.org/10.1371/journal.pone.0061217

Menezes-Blackburn, D., Giles, C., Darch, T., George, T. S., Blackwell, M., Stutter, M., Shand, C., Lumsdon, D., Cooper, P., Wendler, R., Brown, L., Almeida, D. S., Wearing, C., Zhang, H., & Haygarth, P. M. (2018). Opportunities for mobilizing recalcitrant phosphorus from agricultural soils: A review. *Plant and Soil*, *427*(1), 5–16. https://doi.org/10.1007/s11104-017-3362-2

Mousa, W. K., Shearer, C., Limay-Rios, V., Ettinger, C. L., Eisen, J. A., & Raizada, M. N. (2016). Root-hair endophyte stacking in finger millet creates a physicochemical barrier to trap the fungal pathogen Fusarium graminearum. *Nature Microbiology*, *1*(12), 1–12. https://doi.org/10.1038/nmicrobiol.2016.167

Murphy, J., & Riley, J. P. (1962). A modified single solution method for the determination of phosphate in natural waters. *Analytica Chimica Acta*, *27*, 31–36. https://doi.org/10.1016/S0003-2670(00)88444-5

Ober, E. S., Alahmad, S., Cockram, J., Forestan, C., Hickey, L. T., Kant, J., Maccaferri, M., Marr, E., Milner, M., Pinto, F., Rambla, C., Reynolds, M., Salvi, S., Sciara, G., Snowdon, R. J., Thomelin, P., Tuberosa, R., Uauy, C., Voss-Fels, K. P., … Watt, M. (2021). Wheat root systems as a breeding target for climate resilience. *Theoretical and Applied Genetics*, *134*(6), 1645–1662. https://doi.org/10.1007/s00122-021-03819-w

Qi, P.-F., Johnston, A., Balcerzak, M., Rocheleau, H., Harris, L. J., Long, X.-Y., Wei, Y.-M., Zheng, Y.-L., & Ouellet, T. (2012). Effect of salicylic acid on *Fusarium graminearum*, the major causal agent of fusarium head blight in wheat. *Fungal Biology*, *116*(3), 413–426. https://doi.org/10.1016/j.funbio.2012.01.001

Quast, C., Pruesse, E., Yilmaz, P., Gerken, J., Schweer, T., Yarza, P., Peplies, J., & Glöckner, F. O. (2013). The SILVA ribosomal RNA gene database project: Improved data processing and web-based tools. *Nucleic Acids Research*, *41*(D1), D590–D596. https://doi.org/10.1093/nar/gks1219

Quattrone, A., Lopez-Guerrero, M., Yadav, P., Meier, M. A., Russo, S. E., & Weber, K. A. (2024). Interactions between root hairs and the soil microbial community affect the growth of maize seedlings. *Plant, Cell & Environment*, *47*(2), 611–628. https://doi.org/10.1111/pce.14755

R Core Team. (2023). *R: A Language and Environment for Statistical Computing*. R Foundation for Statistical Computing. https://www.R-project.org/

Raymond, N. S., Gómez-Muñoz, B., van der Bom, F. J. T., Nybroe, O., Jensen, L. S., Müller-Stöver, D. S., Oberson, A., & Richardson, A. E. (2021). Phosphate-solubilising microorganisms for improved crop productivity: A critical assessment. *New Phytologist*, *229*(3), 1268–1277. https://doi.org/10.1111/nph.16924

Rengel, Z., Cakmak, I., & White, P. J. (2022). *Marschner's Mineral Nutrition of Plants*. Academic Press.

Richardson, A. E., Lynch, J. P., Ryan, P. R., Delhaize, E., Smith, F. A., Smith, S. E., Harvey, P. R., Ryan, M. H., Veneklaas, E. J., Lambers, H., Oberson, A., Culvenor, R. A., & Simpson,

786 R. J. (2011). Plant and microbial strategies to improve the phosphorus efficiency of
787 agriculture. *Plant and Soil*, *349*(1), 121–156. https://doi.org/10.1007/s11104-011-0950-4

788 Robertson-Albertyn, S., Alegria Terrazas, R., Balbirnie, K., Blank, M., Janiak, A., Szarejko, I.,
789 Chmielewska, B., Karcz, J., Morris, J., Hedley, P. E., George, T. S., & Bulgarelli, D. (2017).
790 Root Hair Mutations Displace the Barley Rhizosphere Microbiota. *Frontiers in Plant Science*,
791 *8*, 1–15. https://doi.org/10.3389/fpls.2017.01094

792 Ruijter, J. M., Ramakers, C., Hoogaars, W. M. H., Karlen, Y., Bakker, O., van den Hoff, M. J.
793 B., & Moorman, A. F. M. (2009). Amplification efficiency: Linking baseline and bias in the
794 analysis of quantitative PCR data. *Nucleic Acids Research*, *37*(6), e45.
795 https://doi.org/10.1093/nar/gkp045

796 Saleem, M., Law, A. D., Sahib, M. R., Pervaiz, Z. H., & Zhang, Q. (2018). Impact of root
797 system architecture on rhizosphere and root microbiome. *Rhizosphere*, *6*(March), 47–51.
798 https://doi.org/10.1016/j.rhisph.2018.02.003

799 Sasse, J., Martinoia, E., & Northen, T. (2018). Feed Your Friends: Do Plant Exudates Shape
800 the Root Microbiome? *Trends in Plant Science*, *23*(1), 25–41.
801 https://doi.org/10.1016/j.tplants.2017.09.003

802 Saunders, W. M. H., & Williams, E. G. (1955). Observations on the Determination of Total
803 Organic Phosphorus in Soils. *Journal of Soil Science*, *6*(2), 254–267.
804 https://doi.org/10.1111/j.1365-2389.1955.tb00849.x

805 Schloss, P. D. (2024). Rarefaction is currently the best approach to control for uneven
806 sequencing effort in amplicon sequence analyses. *mSphere*, *9*(2), e00354-23.
807 https://doi.org/10.1128/msphere.00354-23

808 Seethepalli, A., Dhakal, K., Griffiths, M., Guo, H., Freschet, G. T., & York, L. M. (2021).
809 RhizoVision Explorer: Open-source software for root image analysis and measurement
810 standardization. *AoB PLANTS*, *13*(6), plab056. https://doi.org/10.1093/aobpla/plab056

811 Simpson, R. J., Oberson, A., Culvenor, R. A., Ryan, M. H., Veneklaas, E. J., Lambers, H.,
812 Lynch, J. P., Ryan, P. R., Delhaize, E., Smith, F. A., Smith, S. E., Harvey, P. R., &
813 Richardson, A. E. (2011). Strategies and agronomic interventions to improve the
814 phosphorus-use efficiency of farming systems. *Plant and Soil*, *349*(1), 89–120.
815 https://doi.org/10.1007/s11104-011-0880-1

816 Smith, S. E., & Smith, F. A. (2011). Roles of arbuscular mycorrhizas in plant nutrition and
817 growth: New paradigms from cellular to ecosystem scales. *Annual Review of Plant Biology*,
818 *62*, 227–250. https://doi.org/10.1146/annurev-arplant-042110-103846

819 Suzuki, N., Taketa, S., & Ichii, M. (2003). Morphological and physiological characteristics of
820 a root-hairless mutant in rice (Oryza sativa L.). *Plant and Soil*, *255*(1), 9–17.
821 https://doi.org/10.1023/A:1026180318923

822 Thijs, S., Op De Beeck, M., Beckers, B., Truyens, S., Stevens, V., Van Hamme, J. D.,
823 Weyens, N., & Vangronsveld, J. (2017). Comparative Evaluation of Four Bacteria-Specific
824 Primer Pairs for 16S rRNA Gene Surveys. *Frontiers in Microbiology*, *8*.
825 https://doi.org/10.3389/fmicb.2017.00494

826 Thirkell, T. J., Pastok, D., & Field, K. J. (2020). Carbon for nutrient exchange between
827 arbuscular mycorrhizal fungi and wheat varies according to cultivar and changes in
828 atmospheric carbon dioxide concentration. *Global Change Biology*, *26*(3), 1725–1738.
829 https://doi.org/10.1111/gcb.14851

Tsang, I., Atkinson, J. A., Rawsthorne, S., Cockram, J., & Leigh, F. (2024). Root hairs: An underexplored target for sustainable cereal crop production. *Journal of Experimental Botany*, erae275. https://doi.org/10.1093/jxb/erae275

Tsang, I., Thomelin, P., Ober, E. S., Rawsthorne, S., Atkinson, J. A., Wells, D. M., Percival-Alwyn, L., Leigh, F. J., & Cockram, J. (2024). A novel root hair mutant, srh1, affects root hair elongation and reactive oxygen species levels in wheat. *Frontiers in Plant Science*, *15*. https://doi.org/10.3389/fpls.2024.1490502

Ulén, B., Bechmann, M., Fölster, J., Jarvie, H. P., & Tunney, H. (2007). Agriculture as a phosphorus source for eutrophication in the north-west European countries, Norway, Sweden, United Kingdom and Ireland: A review. *Soil Use and Management*, *23*(s1), 5–15. https://doi.org/10.1111/j.1475-2743.2007.00115.x

Van Kauwenbergh, S. (2010). *World Phosphate Rock Reserves and Resources*. IFDC Publications. https://pdf.usaid.gov/pdf_docs/Pnadw835.PDF

Wang, L., Zhou, J., George, T. S., & Feng, G. (2025). Trade-offs between arbuscular mycorrhizal symbiosis and root hairs in phosphorus source utilization are determined by functional divergence of the rhizosphere bacterial microbiome in barley. *Soil Biology and Biochemistry*, *209*, 109887. https://doi.org/10.1016/j.soilbio.2025.109887

Werner, G. D. A., & Kiers, E. T. (2015). Order of arrival structures arbuscular mycorrhizal colonization of plants. *New Phytologist*, *205*(4), 1515–1524. https://doi.org/10.1111/nph.13092

Wickham, H. (2016). *ggplot2: Elegant Graphics for Data Analysis*. Springer-Verlag New York. https://ggplot2.tidyverse.org

Xiao, J., Dong, S., Shen, H., Li, S., Wessell, K., Liu, S., Li, W., Zhi, Y., Mu, Z., & Li, H. (2022). N Addition Overwhelmed the Effects of P Addition on the Soil C, N, and P Cycling Genes in Alpine Meadow of the Qinghai-Tibetan Plateau. *Frontiers in Plant Science*, *13*. https://doi.org/10.3389/fpls.2022.860590

Yi, H., Hu, S., Zhang, Y., Wang, X., Xia, Z., Lei, Y., & Duan, M. (2023). Proper Delay of Phosphorus Application Promotes Wheat Growth and Nutrient Uptake under Low Phosphorus Condition. *Agriculture*, *13*(4), Article 4. https://doi.org/10.3390/agriculture13040884

Zadoks, J. C., Chang, T. T., & Konzak, C. F. (1974). A decimal code for the growth stages of cereals. *Weed Research*, *14*(6), 415–421. https://doi.org/10.1111/j.1365-3180.1974.tb01084.x

Zhang, C., Simpson, R. J., Kim, C. M., Warthmann, N., Delhaize, E., Dolan, L., Byrne, M. E., Wu, Y., & Ryan, P. R. (2018). Do longer root hairs improve phosphorus uptake? Testing the hypothesis with transgenic Brachypodium distachyon lines overexpressing endogenous genes. *New Phytologist*, *217*(4), 1654–1666. https://doi.org/10.1111/nph.14980

Zhou, J., Zhang, L., Feng, G., & George, T. S. (2022). Arbuscular mycorrhizal fungi have a greater role than root hairs of maize for priming the rhizosphere microbial community and enhancing rhizosphere organic P mineralization. *Soil Biology and Biochemistry*, *171*, 108713. https://doi.org/10.1016/j.soilbio.2022.108713

Zhu, R., Chen, C., Chen, M., Miroslav, V., Dao, J., Xing, Y., Kong, D., Chen, B., & Wang, Z. (2025). How Arbuscular Mycorrhizal Fungi Shape Plant Root Morphology: A Global Meta-Analysis. *Plant, Cell & Environment*. https://doi.org/10.1111/pce.70082

874
875